International Journal of Microscale and Nanoscale Thermal ... ISSN: 1949-4955
Volume 2, Number 4

NON-SIMILAR SOLUTIONS FOR MIXED CONVECTIVE BOUNDARY LAYER FLOW A NON-NEWTONIAN FLUID OVER A WEDGE EMBEDDED IN A POROUS MEDIUM FILLED WITH A NANOFLUID

A. J. Chamkha[1], A. M. Rashad[2], M. A. EL-Hakiem[2], and M. M. M. Abdou[2]

[1]Manufacturing Engineering Department, The Public Authority for Applied Education and Training, Shuweikh, Kuwait

[2]Department of Mathematics, South Valley University, Faculty of Science, Aswan, Egypt

ABSTRACT

The problem of steady, laminar, mixed convection, boundary layer flow of a non-Newtonian power-law fluid over a wedge embedded in a porous medium filled with a nonfluid is considered. The model used for the nanofluid incorporates the effects of Brownian motion and thermophoresis. A mixed convection parameter for the entire range of free-forced-mixed convection is employed and a set of non-similar equations are obtained. These equations are solved numerically by an efficient implicit, iterative, finite-difference method. A parametric study illustrating the influence of the various physical parameters on temperature and nano-particle volume fraction profiles as well as the local Nusselt and Sherwood numbers is conducted. The obtained results are illustrated graphically and the physical aspects of the problem are discussed.

Keywords: Mixed convection, porous media, non-Newtonian fluid, nano-fluids

NOMENCLATURE

C nanoparticle volume fraction
C_w nanoparticle volume fraction at the vertical plate
C_∞ ambient nanoparticle volume fraction attained as y tends to infinity
D_B Brownian diffusion coefficient [m^{-2} s^{-1}]
D_T thermophoretic diffusion coefficient [m^{-2} s^{-1}]
f dimensionless stream function
g gravitational acceleration vector [m s^{-2}]

K permeability of porous medium [m^2]
k_f thermal conductivity [W m^{-1} K^{-1}]
Le Lewis number (equation 14)
N_r Buoyancy Ratio (equation 14)
N_b Brownian motion parameter (equation 14)
N_t thermophoresis parameter (equation 14)
n power-law index
Nu_x local Nusselt number
Pe_x Peclet number
Ra_x local Rayleigh number
Sh_x local Sherwood number
T temperature [K]
T_W temperature at vertical plate [K]
T_∞ ambient temperature attained as y tends to infinity [K]
u,v velocity components [m s^{-1}]
(x,y) Cartesian coordinates [m]

Greek Symbols

α thermal diffusivity of porous medium [m^{-2} s^{-1}]
β volumetric expansion coefficient of fluid [K^{-1}]
χ mixed convection parameter (equation 14)
μ viscosity of fluid [kg m^{-1} s^{-1}]
η,ξ similarity and non-similarity parameters
θ dimensionless temperature
ϕ dimensionless nano-particle volume fraction
ψ stream function
ρ_f fluid density [kg m^{-3}]
ρ_p nano-particle mass density [kg m^{-3}]
$(\rho c)_f$ heat capacity of the fluid [J m^{-3} K^{-1}]
$(\rho c)_p$ effective heat capacity of nano-particle material [J m^{-3} K^{-1}]
τ parameter defined by equation (5)

Subscripts

w conditions at the wall
∞ conditions in the free stream

1. INTRODUCTION

Convective flow in porous media has been widely studied in the recent years due to its wide applications in engineering as geophysical thermal and insulation engineering, the modeling of packed sphere beds, the cooling of electronic systems, groundwater hydrology, chemical catalytic reactors, ceramic processes, grain storage devices, fiber and granular insulation, petroleum reservoirs, coal combustors, ground water pollution and filtration processes, to name just a few of these applications. However, representative studies in this area may be found in the monographs by Nield and Bejan [1], Vafai [2], Pop and Ingham [3], and Ingham and Pop [4]. Also, There has been a sudden surge of interest in heat transfer in non-Newtonian fluids-saturated porous media. This is because in many engineering applications such as a number of fluids exhibiting non-Newtonian behavior come in contact with porous media, particularly in enhanced oil recovery and filtration processes. Further examples of convection of non-Newtonian fluids through porous media may be found in biomechanics, chemical engineering, packed bed reactors, ceramic engineering applications such as drying or burnout of binder systems from green compacts during colloidal processing of ceramics; and the production of heavy crude oil by means of thermal methods, such as steam injection into an oil reservoir. Chen and Chen [5] have presented similarity solutions for free convection of non-Newtonian fluids over vertical surfaces in porous media. Mehta and Rao [6] have investigated buoyancy induced flow of non-Newtonian fluids over a non-isothermal horizontal plate embedded in a porous medium. Jumah and Mujumdar [7] have considered free convection heat and mass transfer of non-Newtonian power-law fluids with yield stress from a vertical flat plate in saturated porous medium. Recently, Chamkha and Al-Humoud [8] have considered mixed convection heat and mass transfer of non- Newtonian fluids from a permeable surface embedded in a porous medium. consider coupled heat and mass transfer by mixed convection for a non-Newtonian power-law fluid flow over a permeable wedge embedded in a fluid-saturated porous medium. The problem of coupled heat and mass transfer by mixed convective flow of a non- Newtonian power-law fluid over a permeable wedge embedded in a porous medium is considered by Chamkha [9]. EL-Kabeir et al. [10] considered the coupled heat and mass transfer by mixed convection stagnation-point flow of a power-law non-Newtonian fluid towards a stretching surface in the presence of thermal-diffusion and diffusion-thermo effects.

However, it is well known that conventional heat transfer fluids, including oil, water, and ethylene glycol mixture are poor heat transfer fluids, since the thermal conductivity of these fluids plays an important role on the heat transfer coefficient between the heat transfer medium and the heat transfer surface. An innovative technique for improving heat transfer by using ultra fine solid particles in the fluids has been used extensively during the last several years. The term nanofluid refers to these kinds of fluids by suspending nano-scale particles in the base fluid and has been introduced by Choi [11]. Daungthongsuk and Wongwises [12] studied the influence of thermophysical properties of nanofluids on the convective heat transfer and summarized various models used in literature for predicting the thermophysical properties of nanofluids. Thermal Instability in a Porous Medium Layer Saturated by a Nanofluid investigated by Nield and Kuznetsov [13]. Abu-Nada and Oztop [14] have studied effects of inclination angle on natural convection in enclosures filled with Cu-water nanofluid. Nield and Kuznetsov [15] have suggested natural convective boundary-layer flow

of a nanofluid past a vertical plate. Chamkha et al. [16] studied the mixed convection MHD flow of a nanofluid past a stretching permeable surface in the presence of Brownian motion and thermopherosis effects. Chamkha et al. [17] have also analyzed the natural convection past a sphere embedded in a porous medium saturated by a nanofluid. Gorla et al. [18] studied the steady boundary layer flow of a nanofluid on a stretching circular cylinder in a stagnant free stream.

The objective of this paper is to study the mixed convection boundary layer flow of a non-Newtonian power-law fluid flow over a wedge embedded in a fluid-saturated porous medium filled with a nanofluid is considered. The model used for the nanofluid incorporates the effects of Brownian motion and thermophoresis in the entire range of free-forced-mixed convection parameter. A parametric study illustrating the influence of the various physical parameters on temperature and nano-particle volume fraction profiles as well as the local Nusselt and Sherwood numbers is conducted. The obtained results are illustrated graphically and the physical aspects of the problem are discussed.

2. PROBLEM FORMULATION

Consider steady mixed convective boundary-layer flow of a non-Newtonian power-law fluid over a wedge embedded in a porous medium filled with nanofluid. The model used for the nanofluid incorporates the effects of Brownian motion and thermophoresis. The wedge surface is maintained at a constant temperature T_w and a constant nano-particle volume fraction C_w and the ambient temperature and nano-particle volume fraction far away from the surface of the wedge T_∞ and C_∞ are assumed to be uniform. For $T_w>T_\infty$ and $C_w>C_\infty$ an upward flow is induced as a result of the thermal and nano-particle volume fraction buoyancy effects. The flow over the wedge is assumed to be two-dimensional, laminar, steady, and incompressible. Figure 1 shows the flow model and the physical coordinate system. The power-law model of Ostwald-de-Waele which is adequate for many non-Newtonian fluids is considered in the present work. The porous medium is assumed to be uniform, isotropic and in local thermal equilibrium with the fluid. All fluid properties are assumed to be constant. Under the Boussinesq and boundary-layer approximations, the governing equations for this problem can be written as:

$$\frac{\partial u}{\partial x}+\frac{\partial v}{\partial y}=0\,, \tag{1}$$

$$nu^{n-1}\frac{\partial u}{\partial y}=\frac{(1-C_\infty)\rho_{f\infty}\beta gK}{\mu}\frac{\partial T}{\partial y}-\frac{(\rho_p-\rho_{f\infty})gK}{\mu}\frac{\partial C}{\partial y}\,, \tag{2}$$

$$u\frac{\partial T}{\partial x}+v\frac{\partial T}{\partial y}=\alpha_e\frac{\partial^2 T}{\partial y^2}+\tau\left[D_B\frac{\partial C}{\partial y}\frac{\partial T}{\partial y}+\left(\frac{D_T}{T_\infty}\right)\left(\frac{\partial T}{\partial y}\right)^2\right], \tag{3}$$

$$\frac{1}{\varepsilon}\left(u\frac{\partial C}{\partial x}+v\frac{\partial C}{\partial y}\right)=D_B\frac{\partial^2 C}{\partial y^2}+\left(\frac{D_T}{T_\infty}\right)\frac{\partial^2 T}{\partial y^2}, \tag{4}$$

where x and y denote the vertical and horizontal directions, respectively. u, v, T and C are the x- and y components of velocity, temperature and nano-particle volume fraction, respectively. K, β, g, D_B and D_T are the modified permeability of the porous medium, volumetric expansion coefficient of fluid, gravitational acceleration vector, Brownian diffusion coefficient and thermophoretic diffusion coefficient, respectively. n, μ, ρ_f and ρ_p are the power-law fluid viscosity index, consistency index for viscosity, fluid density and nano-particle mass density, respectively. $\alpha_e = k/(\rho c)_f$ and $\tau = (\rho c)_p/(\rho c)_f$ are the thermal diffusivity of porous medium and the ratio of heat capacities, respectively. k, $(\rho c)_f$ and $(\rho c)_p$ are thermal conductivity, heat capacity of the fluid and the effective heat capacity of nano-particle material, respectively.

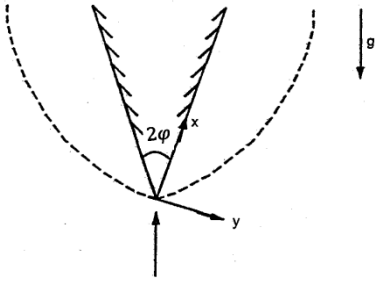

Figure 1. Flow Model and Coordinate System.

The modified permeability of the porous medium K for flows of non-Newtonian power-law fluids is given by:

$$K=\frac{1}{2C_t}\left(\frac{n\varepsilon}{3n+1}\right)^n\left(\frac{50k^*}{3\varepsilon}\right)^{(n+1)/2}, \tag{5}$$

$$k^*=\frac{\varepsilon^3 d^2}{150(1-\varepsilon)^2}, \tag{6}$$

$$C_t=\begin{cases}\dfrac{25}{12}, & \text{Christopher and Middleman [19]}\\ \dfrac{2}{3}\left(\dfrac{8n}{9n+3}\right)\left(\dfrac{10n-3}{6n+1}\right)\left(\dfrac{75}{16}\right)^{3(10n-3)/(10n+11)}, & \text{Dharmadhikari and Kale [20]}\end{cases} \tag{7}$$

where ε and d is the porosity and the particle diameter of the packed-bed porous medium.

The boundary conditions suggested by the physics of the problem are given by

$$y = 0: \quad v(x,0) = 0, \quad T = T_w, \quad C = C_w, \tag{8a}$$

$$y \to \infty: \quad u = U_\infty, \quad T = T_\infty, \quad C = C_\infty, \tag{8b}$$

where T_w and C_w are the wall temperature and wall nano-particle volume fraction, respectively. U_∞, T_∞ and C_∞ are the free stream velocity, temperature and nano-particle volume fraction, respectively.

It is convenient to transform the governing equations into a non-similar dimensionless form which can be suitable for solution as an initial-value problem. This can be done by introducing the stream function such that: $u = \partial\psi / \partial y$,$v = -\partial\psi / \partial x$ and using

$$\eta = \frac{y}{x}(Pe_x^{1/2})\chi^{-1},\ \psi = \alpha_e (Pe_x^{1/2})\chi^{-1} f(\chi,\eta),\ \theta = \frac{T - T_\infty}{T_w - T_\infty},\ \phi = \frac{C - C_\infty}{C_w - C_\infty},$$

$$m = \frac{\varphi}{\pi - \varphi},\ U_\infty = ax^m,\ Pe_x = U_\infty x / \alpha_e,$$

$$Ra_x = (x / \alpha_e)\left\{(1 - C_\infty)\rho_{f\infty} g \beta_T \mathrm{K}(T_w - T_\infty)/\mu\right\}^{\frac{1}{n}} \tag{9}$$

where Pe_x and Ra_x are the local Peclet and modified Rayleigh numbers, respectively. The parameters a, φ and m are a free stream velocity constant, half-wedge angle and the free stream velocity exponent, respectively. Substituting Eqs. (9) into Eqs. (1) through (4) produces the following non-similar equations:

$$nf'^{n-1} f'' = (1-\chi)^{2n}(\theta' - N_r \phi'), \tag{10}$$

$$\theta'' + \frac{1}{2}(1 + m\chi) f \theta' + N_b \phi' \theta' + N_t \theta'^2 = \frac{1}{2} m\chi(1-\chi)(f' \frac{\partial\theta}{\partial\chi} - \theta' \frac{\partial f}{\partial\chi}), \tag{11}$$

$$\phi'' + \frac{Le}{2}(1 + m\chi) f \phi' + \frac{N_t}{N_b}\theta'' = \frac{Le}{2} m\chi(1-\chi)(f' \frac{\partial\phi}{\partial\chi} - \phi' \frac{\partial f}{\partial\chi}), \tag{12}$$

$$(1 + m\chi) f(\chi,0) - m\chi(1-\chi)\frac{\partial f}{\partial\chi}(\chi,0) = 0,\ \theta(\chi,0) = 1,\ \phi(\chi,0) = 1, \tag{13a}$$

$$f'(\chi,\infty) = \chi^2,\ \theta(\chi,\infty) = 0,\ \phi(\chi,\infty) = 0 \tag{13b}$$

where $Le = \frac{\alpha_e}{D_B}$, $N_r = \frac{(\rho_p - \rho_{f\infty})(C_w - C_\infty)}{(1-C_\infty)\rho_{f\infty}\beta(T_w - T_\infty)}$, $N_b = \frac{\varepsilon(\rho c)_p D_B (C_w - C_\infty)}{(\rho c)_f \alpha_e}$,

$N_t = \frac{\varepsilon(\rho c)_p D_T (T_w - T_\infty)}{(\rho c)_f \alpha_e T_\infty}$, $\chi = \left[1 + \sqrt{Ra_x / Pe_x}\right]^{-1}$, (14)

are the Lewis number, buoyancy ratio, Brownian motion parameter, thermophoresis parameter and mixed convection parameter, respectively. It should be noted that $\chi = 0$ ($Pe_x = 0$) corresponds to pure free convection while $\chi = 1$ ($Ra_x = 0$) corresponds to pure forced convection. The entire regime of mixed convection corresponds to values of χ between 0 and 1. Of special significance for this problem are the local Nusselt and Sherwood numbers. These physical quantities can be defined as:

$$Nu_x = -(Pe_x)^{1/2} \chi^{-1} \theta'(\chi, 0) \ , \tag{15}$$

$$Sh_x = -(Pe_x)^{1/2} \chi^{-1} \phi'(\chi, 0) \, . \tag{16}$$

3. NUMERICAL METHOD AND VALIDATION

Equations (10) through (13) represent an initial-value problem with χ playing the role of time. This general non-linear problem can not be solved in closed form and, therefore, a numerical solution is necessary to describe the physics of the problem. The implicit, tridiagonal finite-difference method similar to that discussed by Blottner [21] has proven to be adequate and sufficiently accurate for the solution of this kind of problems. Therefore, it is adopted in the present work. All first-order derivatives with respect to χ are replaced by two-point backward-difference formulae when marching in the positive χ direction and by two-point forward-difference formulae when marching in the negative ξ direction. Then, all second-order differential equations in η are discretized using three-point central difference quotients.

This discretization process produces a tri-diagonal set of algebraic equations at each line of constant χ which is readily solved by the well known Thomas algorithm (see Blottner [21]). During the solution, iteration is employed to deal with the nonlinearity aspect of the governing differential equations. The problem is solved line by line starting with line χ=0 where similarity equations are solved to obtain the initial profiles of velocity, temperature and concentration and marching forward (or backward) in χ until the desired line of constant χ is reached. Variable step sizes in the η direction with $\Delta\eta_1 = 0.001$ and a growth factor G = 1.035 such that $\Delta\eta_n = G\Delta\eta_{n-1}$ and constant step sizes in the χ direction with $\Delta\chi = 0.01$ are employed. These step sizes are arrived at after many numerical experimentations performed to assess grid independence. The convergence criterion employed in the present work is based on the difference between the current and the previous iterations. When this difference reached 10^{-5} for all points in the η directions, the solution was assumed converged and the iteration process was terminated.

4. RESULTS AND DISCUSSION

In this section, a representative set of graphical results for the dimensionless velocity $f'(\xi,\eta)$, temperature $\theta(\xi,\eta)$, and nano-particle volume fraction $\phi(\xi,\eta)$ as well as the reduced local Nusselt number Nu = $-\theta'(\chi,0)$, and the reduced local Sherwood number Sh = $-C'(\chi,0)$ is presented and discussed for various parametric conditions. These conditions are intended for various values of and the power-law fluid viscosity index n, buoyancy ratio Nr, Lewis number Le, thermophoresis parameter Nt, Brownian motion parameter Nb, free stream velocity exponent m and mixed convection parameter χ, respectively.

Figures 2(a) through 2(c) present the effects of the fluid power-law index n on the velocity f', temperature θ and nano-particle volume fraction ϕ, respectively. It can be seen that the velocity profile for shear-thickening or dilatant fluids ($1<n<2$) is larger than that for shear-thinning or pseudo-plastic fluids ($0<n<1$), i.e., the effect of increasing the values of the power-law index parameter n is to decrease the velocity, while the fluid temperature and volume fraction profiles as well as their boundary layers increase.

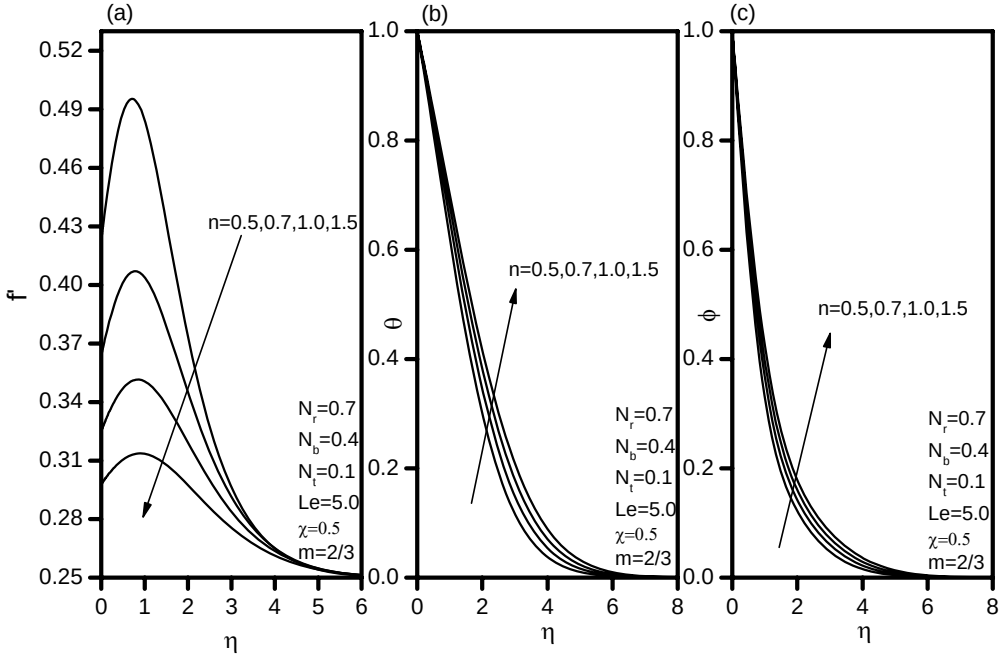

Figure 2. Effects of n on the (a) velocity, (b) temperature, (c) volume fraction profiles.

Figures 3 and 4 illustrate the influence of the fluid power-law index n in the entire range of the mixed convection parameter $0 \le \chi \le 1$ on the reduced local Nusselt number [Nu = $-\theta'(\chi,0)$] and the reduced local Sherwood number [Sh = $-C'(\chi,0)$] for power-law fluid viscosity indices n=0.7 (shear-thinning or pseudo-plastic fluid), n=1.0 (Newtonian fluid) and n=1.5 (shear-thickening or dilatant fluid), respectively. In general, the local Nusselt and Sherwood numbers decrease as the power-law fluid index n increases. However, this is not true for all values of χ. It is predicted that, the values of Nu and Sh increase as n increases for

small values of χ (for example $\chi<0.35$) while the local Nusselt and Sherwood numbers decrease with increasing values of n in the rest of the range (for example $0.35<\chi<1$), the local Nusselt and Sherwood numbers remains almost unchanged for all values of n at $\chi=1$ (forced convection limit). All these features are clear from Figures 3 and 4.

The effects of the buoyancy ratio N_r on the velocity and temperature and nano-particle volume fraction profiles are presented in Figs. 5(a)-5(c), respectively. In general, increases in the value of N_r have the tendency to cause more resistance flow along the wedge surface which filled with nanofluids. This behavior in the flow velocity is accompanied by slight increases in the fluid temperature and volume fraction as well as increases in their boundary layers as N_r increases from 0.1 to 0.7.

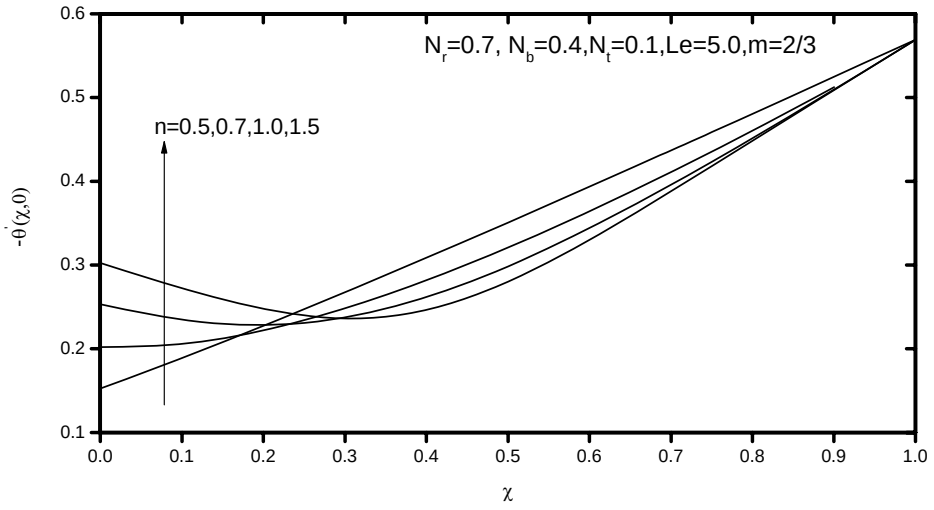

Figure 3. Effects of n on the local Nusselt number.

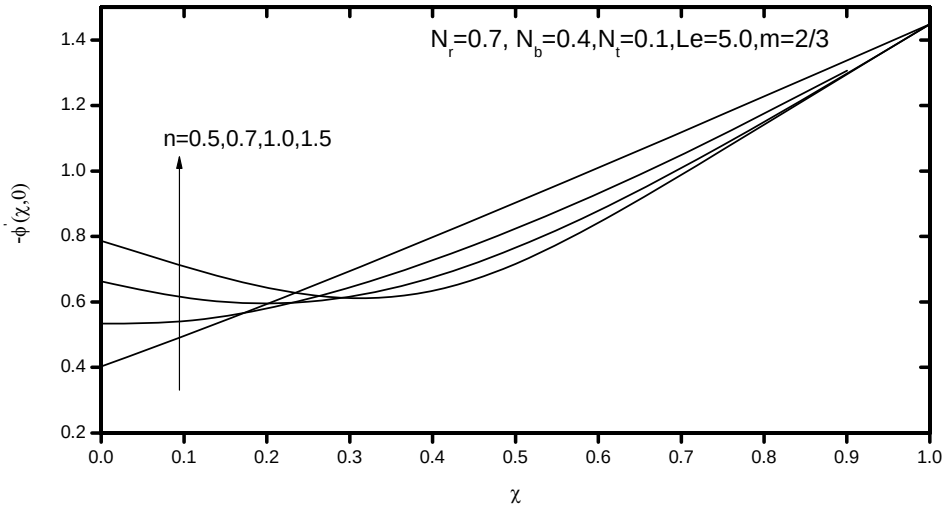

Figure 4. Effects of n on the local Sherwood number.

On the other hand, Figures 6 and 7 illustrate the influence of the buoyancy ratio N_r in the entire range of the mixed convection parameter $0 \le \chi \le 1$ on the reduced local Nusselt number [Nu = –θ'(χ,0)] and the reduced local Sherwood number [Sh = –C'(χ,0)] for power-law fluid viscosity indices n=1.5 (shear-thickening or dilatant fluid), respectively.

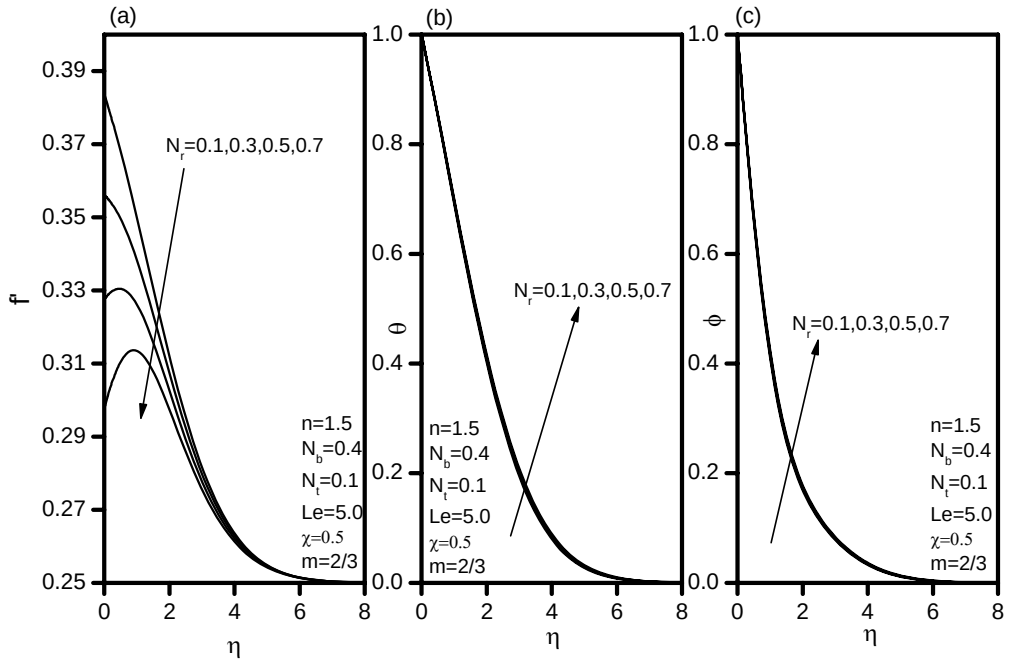

Figure 5. Effects of Nr on the (a) velocity, (b) temperature, (c) volume fraction profiles.

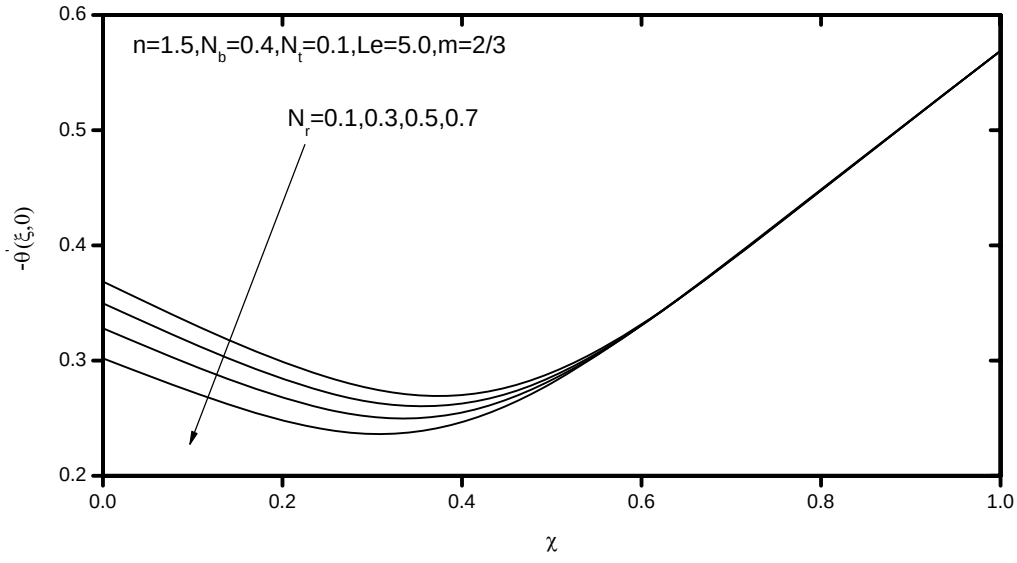

Figure 6. Effects of Nr on the local Nusselt number.

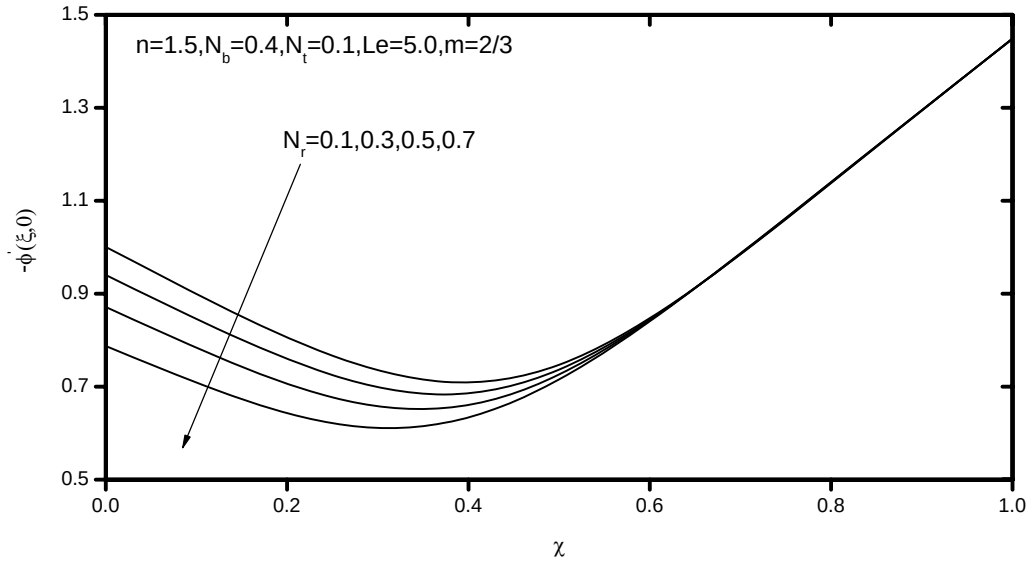

Figure 7. Effects of Nr on the local Sherwood number.

The increases in the fluid temperature and volume fraction profiles as Nr increases mentioned above causes the negative values of the wall temperature and volume fraction slopes to decrease yielding increases in both the local Nusselt and Sherwood numbers in the entire range of mixed convection parameter $0<\chi<1$. However, for $\chi=1$ (forced convection limit), the flow is uncoupled from the thermal and volume fraction buoyancy effects and therefore, the local Nusselt and Sherwood numbers are constant for all values of N_r. From the definition of χ, it is seen that increases in the value of the parameter Ra_x/Pe_x causes the mixed convection parameter χ to decrease. Thus, small values of Ra_x/Pe_x correspond to values of χ close to unity which indicate almost pure forced convection regime. On the other hand, high values of Ra_x/Pe_x correspond to values of χ close to zero which indicate almost pure free convection regime. Furthermore, moderate values of Ra_x/Pe_x represent values of χ between 0 and 1 which correspond to the mixed convection regime. For the forced convection limit (χ = 1) it is clear from Eq. (10) that the velocity in the boundary layer f' is uniform irregardless of the value of n. However, for smaller values of χ (higher values of Ra_x/Pe_x) at a fixed value of N_r and n=1.0, the buoyancy effect increases. As this occurs, the fluid velocity close to the wall increases for values of $\chi < 0.5$ due to the buoyancy effect which becomes maximum for $\chi = 0$ (free convection limit). This decrease and increase in the fluid velocity f' as χ is decreased from unity to zero is accompanied by a respective increase and a decrease in the fluid temperature and concentration. As a result, the local Nusselt and Sherwood numbers tend to decrease and then increase as χ is increased from 0 to unity forming slight dips. This result quantitatively with the expectations in Chamkha [9].

Figures 8(a)-8(c) show the representative temperature and nano-particle volume fraction profiles for different values of Lewis number Le, respectively. It is clearly observed that the velocity increases while both the fluid temperature and volume fraction as well as its boundary-layer thickness decrease considerable as the Lewis number Le increases. This yields enhancements in both heat and mass transfer effects.

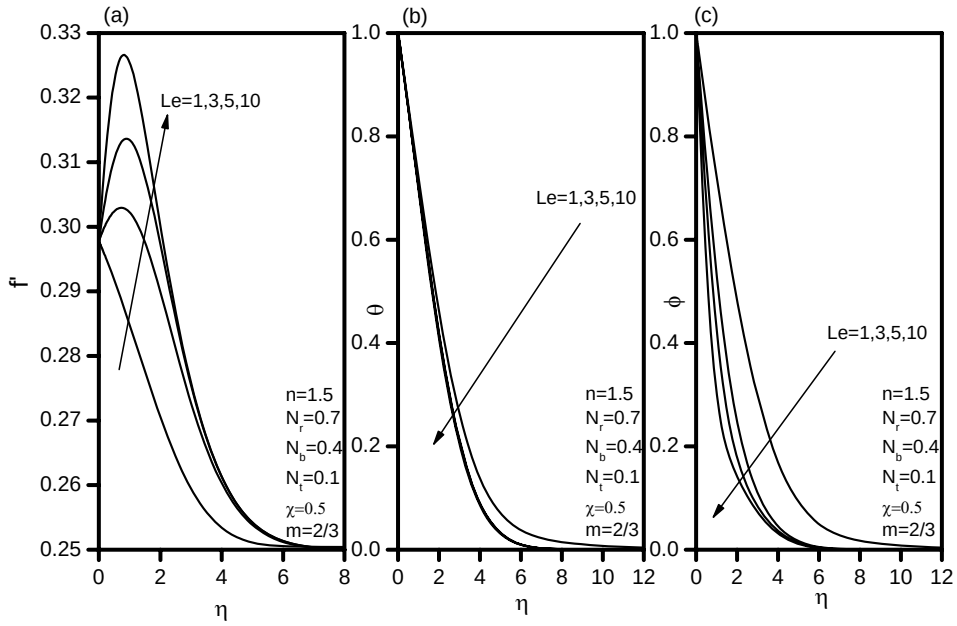

Figure 8. Effects of Le on the (a) velocity, (b) temperature, (c) volume fraction profiles.

Figures 9 and 10 present the effects of the Lewis number Le on the reduced local Nusselt number Nu and reduced local Sherwood number Sh in the entire range $0 \le \chi \le 1$, respectively. As mentioned before, increasing the Lewis number Le causes enhancements in both the heat and mass transfer effects represented by increases in the reduced local Sherwood number in the entire range $0 \le \chi \le 1$, while the reduced local Nusselt number increases for values of $\chi < 0.5$ and it decreases in the entire range $0.5 < \chi \le 1$ with increasing values of Le.

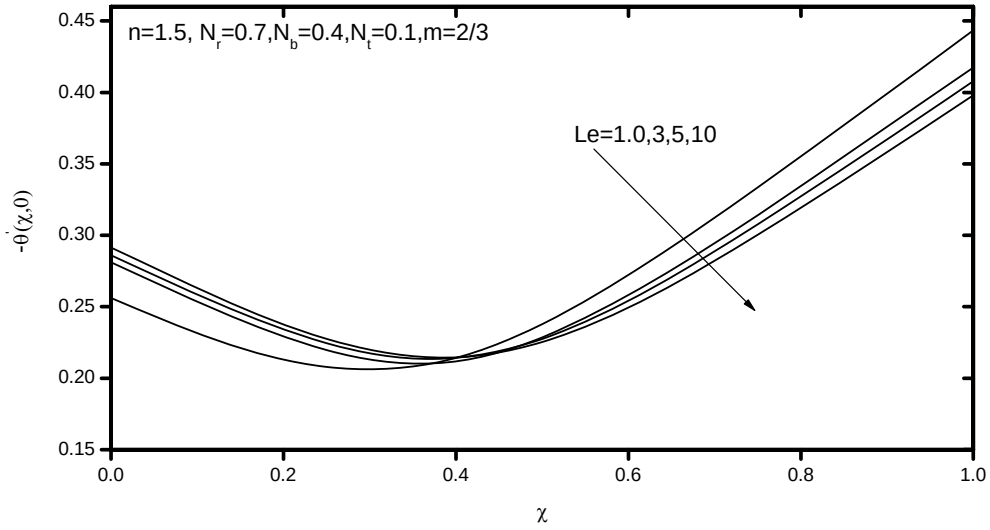

Figure 9. Effects of Le on the local Nusselt number.

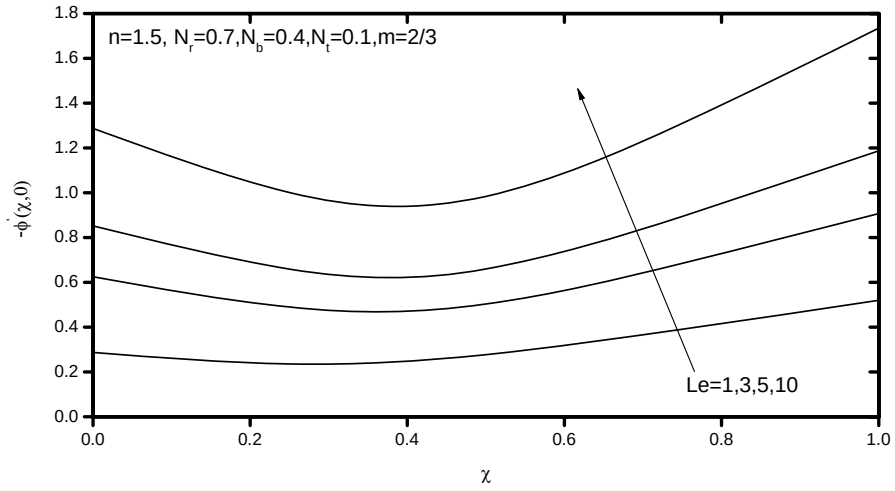

Figure 10. Effects of Le on the local Sherwood number.

Figures 11(a)-11(c) display typical velocity, temperature and nano-particle volume fraction profiles for various values of thermophoresis parameter N_t, respectively. Increases in the thermophoresis parameter N_t have the tendency to decrease the velocity profiles while increase both the fluid temperature and volume fraction profiles. Figures 12 and 13 depict the influence of the thermophoresis parameter N_t on the values of Nu and Sh in the entire mixed convection range $0 \le \chi \le 1$, respectively. Increasing the value of the thermophoresis parameter N_t results in increasing both the temperature and volume fraction profiles causing the values of Nu and Sh to decrease, respectively as N_t increases.

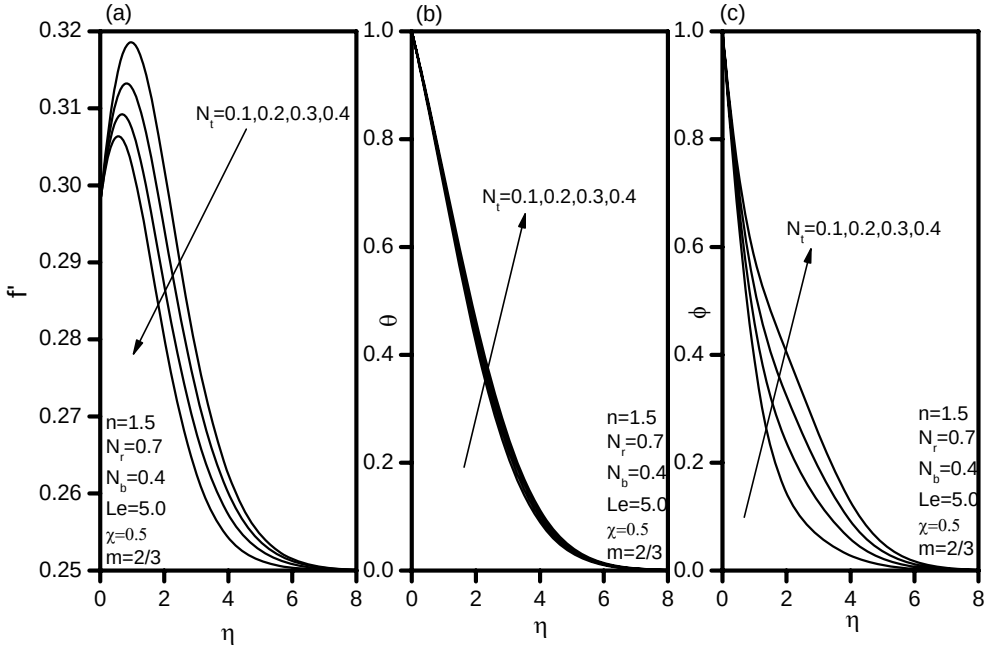

Figure 11. Effects of Nt on the (a) velocity, (b) temperature, (c) volume fraction profiles.

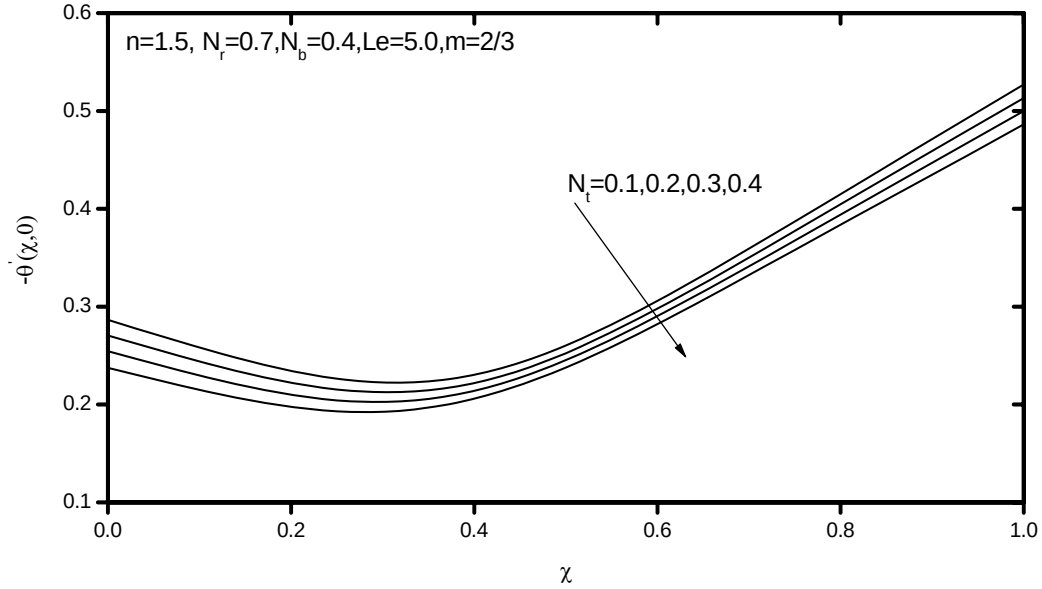

Figure 12. Effects of Nt on the local Nusselt number.

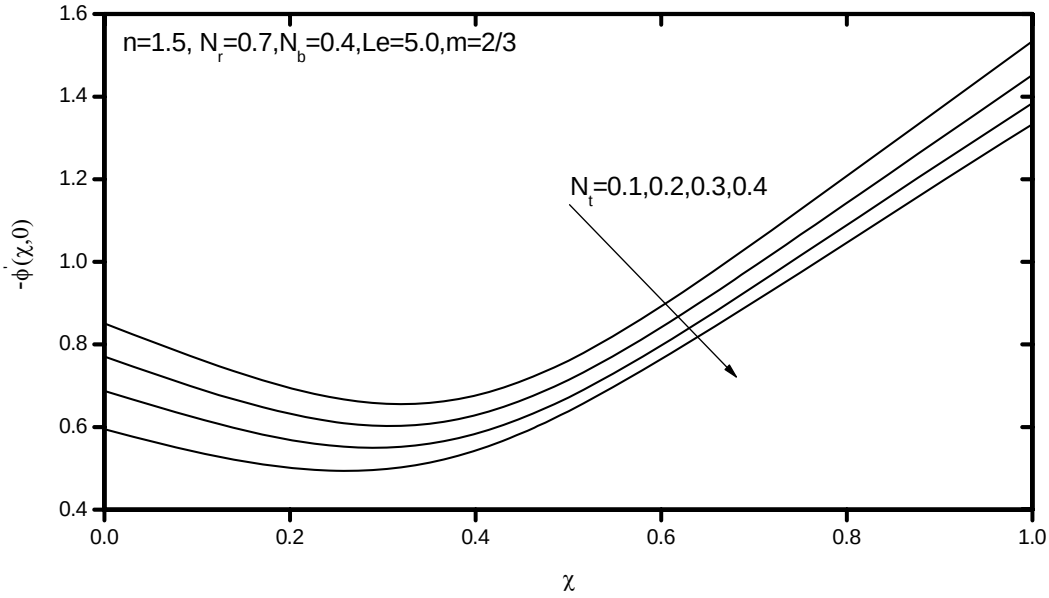

Figure 13. Effects of Nt on the local Sherwood number.

Figures 14(a)-14(c) show the effects of increasing the Brownian motion parameter N_b on the velocity, temperature and volume fraction profiles, respectively. It can be seen that the increasing the value of the Brownian motion parameter N_b causes increases in both of the velocity and volume fraction profiles with insignificant decrease on the distribution of the fluid temperature. These behaviors are clearly shown in Figures 14(a)-14(c).

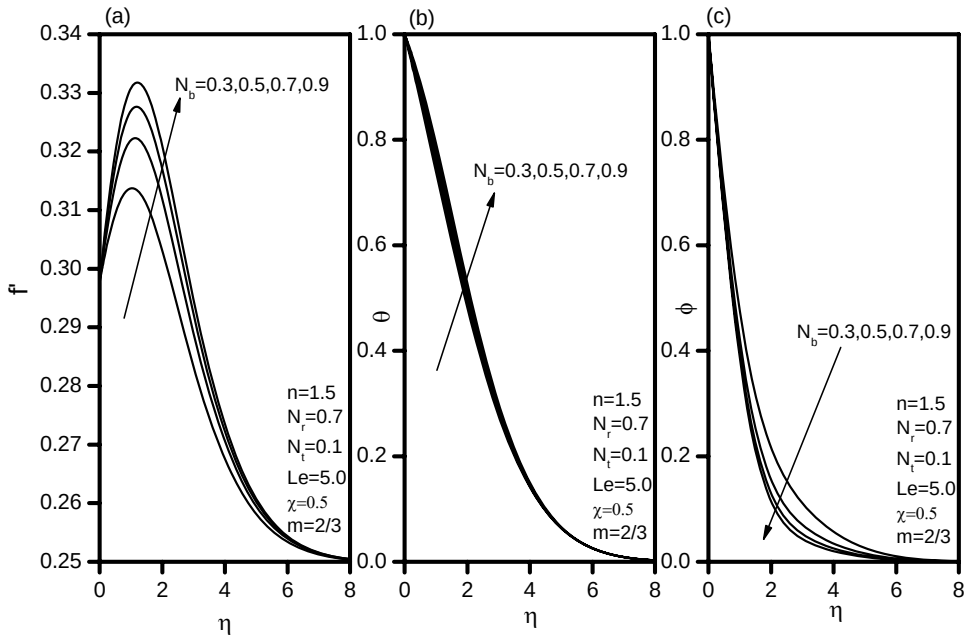

Figure 14. Effects of Nb on the (a) velocity, (b) temperature, (c) volume fraction profiles.

Figures 15 and 16 present the effects of the Brownian motion parameter N_b on the reduced local Nusselt number Nu and reduced local Sherwood number Sh in the entire range $0 \le \chi \le 1$, respectively. As indicated before, increasing the Brownian motion parameter N_b causes increasing in the volume fraction profiles while its temperature decrease causing the negative wall slope of volume fraction profiles to decrease while the negative wall slope of temperature to increase. This yields reduction in the local Sherwood number and enhancement in the local Nusselt number.

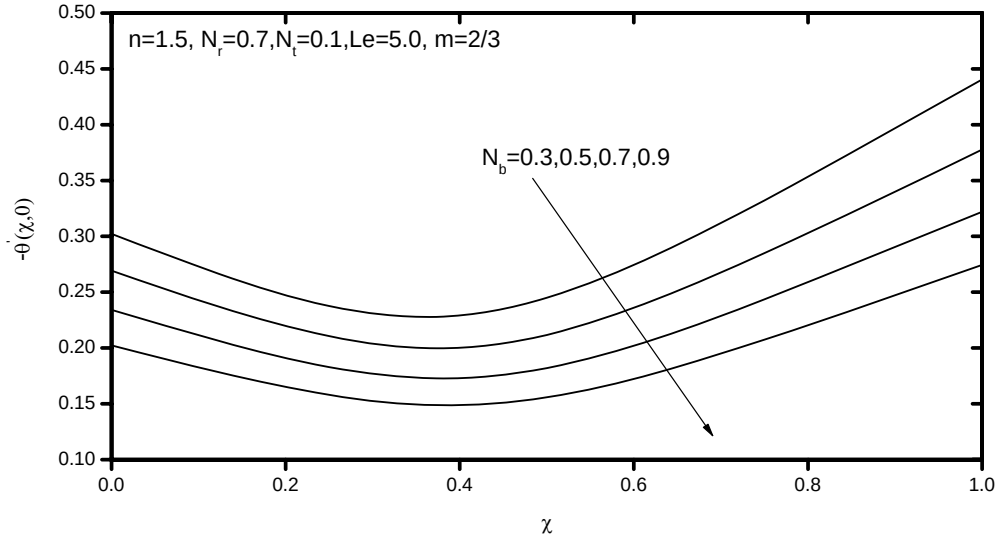

Figure 15. Effects of Nb on the local Nusselt number.

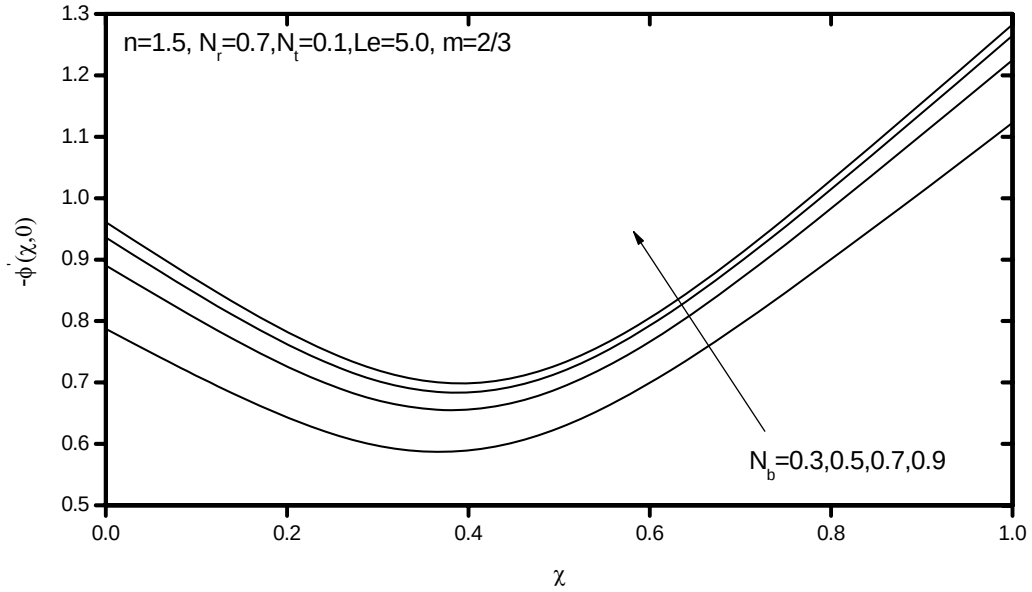

Figure 16. Effects of Nb on the local Sherwood number.

Finally, Figures 17(a)-17(c) depict the effects of the free stream velocity exponent m on the velocity, temperature and nano-particle volume fraction profiles, respectively.

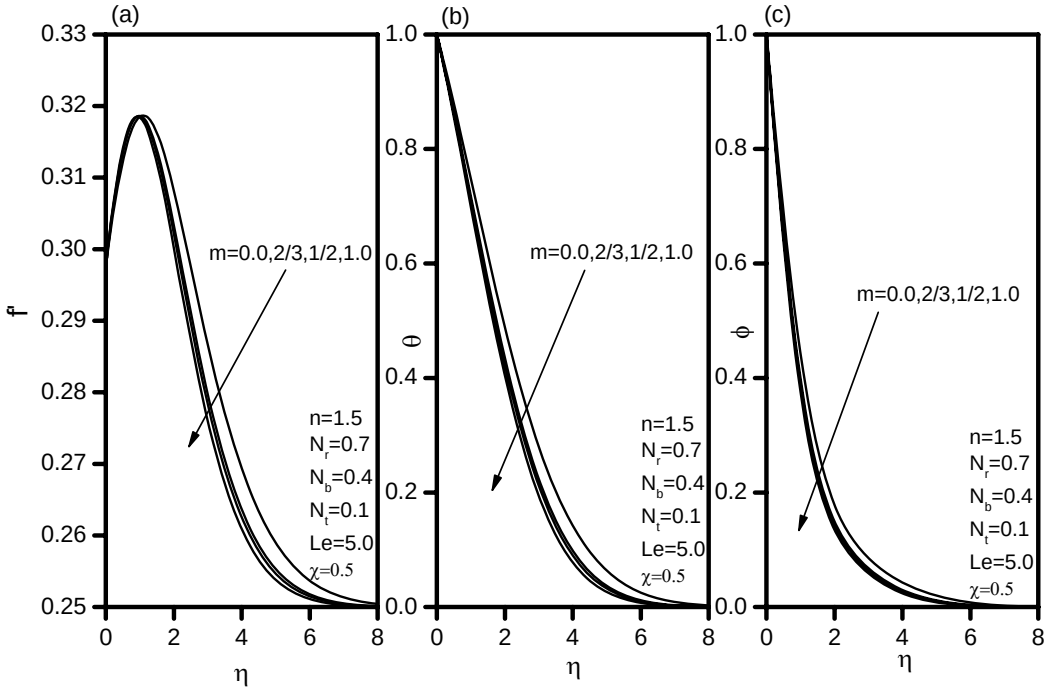

Figure 17. Effects of m on the (a) velocity, (b) temperature, (c) volume fraction profiles.

It is observed that as the value of m increases, either of the velocity, fluid temperature and volume fraction profiles decrease with slight effect of their boundary-layer thicknesses. On other hand, Figures 18 and 19 illustrate the effects of the free stream velocity exponent m on the values of the reduced local Nusselt and Sherwood numbers (Nu and Sh) in the range $0 \le \chi \le 1$, respectively. It is observed that the reduced local Nusselt and Sherwood numbers increase as the value of m increases. In addition, the effect of m is very small for small values of χ and becomes more pronounced as χ increases reaching its maximum at χ=1.

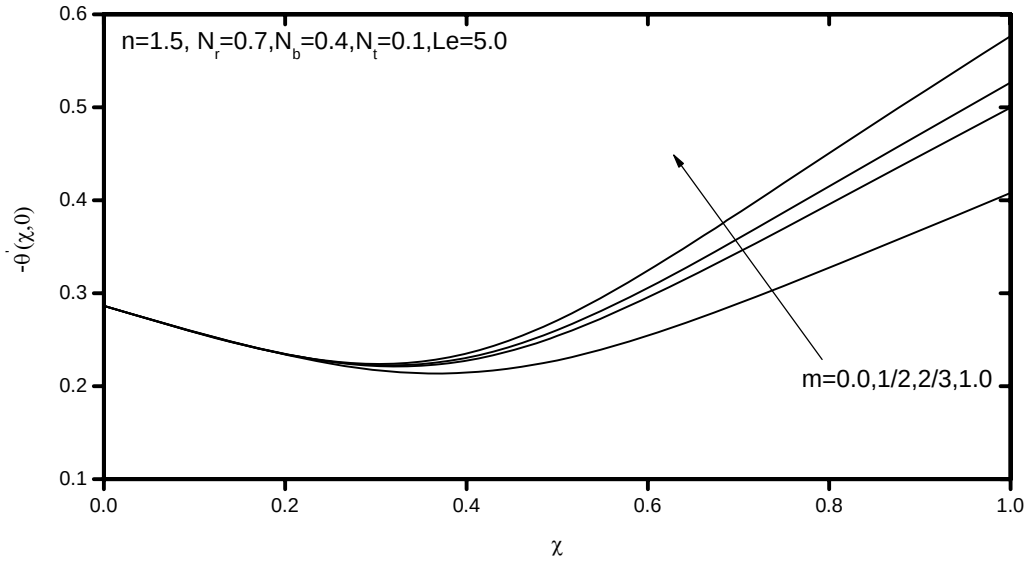

Figure 18. Effects of m on the local Nusselt number.

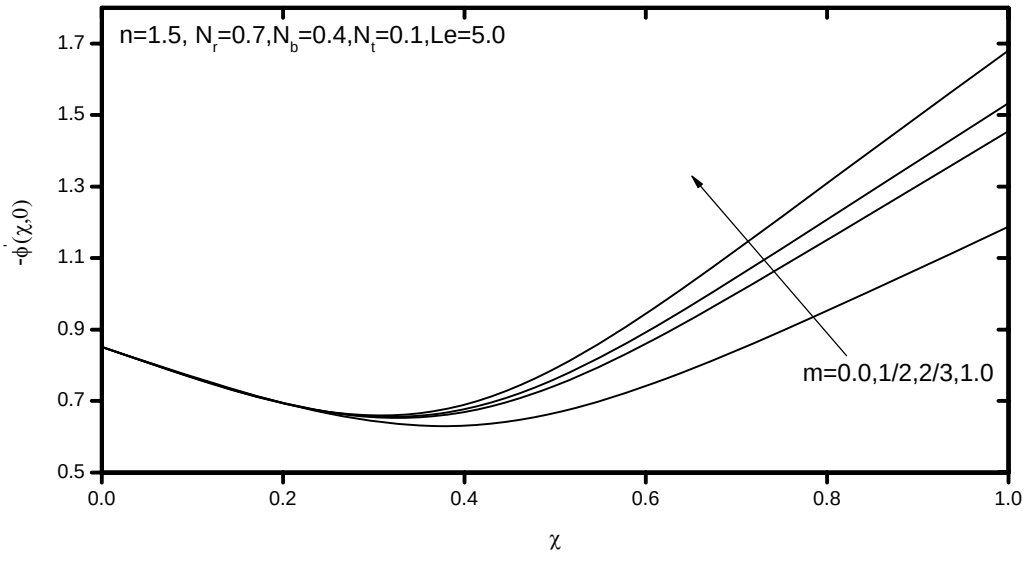

Figure 19. Effects of m on the local Sherwood number.

CONCLUSION

In the present work, we have studied theoretically the problem of steady mixed convective boundary layer flow of a non-Newtonian power-law fluid over a wedge embedded in a porous medium filled with nanofluids. The model used for the nanofluid incorporates the effects of Brownian motion and thermophoresis and a single parameter for the entire range of free-forced-mixed convection regime was employed. The obtained non-similar differential equations were solved numerically by an efficient implicit finite-difference method. The results focused on the effects of the power-law fluid viscosity index, buoyancy ratio, Lewis number, thermophoresis parameter, Brownian motion parameter, free stream velocity exponent and mixed convection parameter on the reduced local Nusselt and Sherwood numbers. It was found that as the power-law fluid index was increased, both the reduced local Nusselt and Sherwood numbers increased in the entire range of free and for small values of mixed convection parameter but it produces the opposite effect in the rest of the range mixed convection regime, while they remained constant for the forced-convection regime for all power-law fluid index values. In addition, it was concluded that as the buoyancy ratio was increased, both the reduced local Nusselt and Sherwood numbers decreased in the entire range of free and mixed convection regime while they remained constant for the forced-convection regime. However, they decreased and then increased forming dips as the mixed convection parameter was increased from the free convection limit to the forced-convection limit. Also, increasing the Lewis number produced increases in the reduced local Sherwood number in the entire range of the mixed convection regime, while the reduced local Nusselt number increase in the entire range of free regime and small value of mixed convection, and it decreases in the entire range of forced regime and large value of mixed convection with increasing values of Lewis number. Furthermore, both of the reduced local Nusselt and Sherwood numbers increased as the free stream velocity exponent increased. Moreover, the reduced local Nusselt and Sherwood numbers decreased as the thermophoresis parameter increased whereas the reduced local Nusselt number decreased and the reduced local Sherwood number increased as the Brownian motion parameter increased.

REFERENCES

[1] D.A. Nield, A. Bejan, *Convection in Porous Media*, third Ed., Springer, New York, (2006).

[2] K. Vafai (Ed.), Handbook of Porous Media, Marcel Dekker, Marcel, (2000).

[3] Pop, D.B. Ingham, *Convective Heat Transfer: mathematical and computational modelling of viscous fluids and porous media*, Pergamon, Oxford, (2001).

[4] D.B. Ingham, I. Pop (Eds.), *Transport Phenomena in Porous Media*, Pergamon, Oxford, (1998), vol. II, (2002).

[5] H.T. Chen, C.K. Chen, Free convection of non-Newtonian fluids along a vertical plate embedded in a porous medium, Trans. ASME, *J. Heat Transfer* 110 (1988) 257-260.

[6] K.N. Mehta, K.N. Rao, Buoyancy-induced flow of non-Newtonian fluids over a non-isothermal horizontal plate embedded in a porous medium, *Int. J. Eng. Sci*. 32 (1994) 521-525.

[7] R.Y. Jumah, A.S. Mujumdar, Free convection heat and mass transfer of non-Newtonian power law fluids with yield stress from a vertical flat plate in saturated porous media, *Int. Commun. Heat Mass Transfer 27* (2000) 485-494.

[8] A.J. Chamkha, J. Al-Humoud, Mixed convection heat and mass transfer of non-Newtonian fluids from a permeable surface embedded in a porous medium, Int. J. Numer. Meth. *Heat and Fluid Flow* 17 (2007) 195-212.

[9] Ali J. Chamkha, Heat and mass transfer of a non-newtonian fluid flow over a permeable wedge in porous media with variable wall temperature and concentration and heat source or sink, *WSEAS Transactions On Heat And Mass Transfer* 5 (1) (2010) 11-20.

[10] S.M.M. EL-Kabeir, A.J. Chamkha, A.M. Rashad, Heat and mass transfer by MHD stagnation-point flow of a power-law fluid towards a stretching surface with radiation, chemical reaction and Soret and Dufour effects, *International Journal Of Chemical Reactor Engineering* 8 (2010) 1-18.

[11] S.U.S. Choi, Enhancing thermal conductivity of fluids with nanoparticle. in: D.A. Siginer, H.P. Wang (Eds.), Developments and Applications of Non-Newtonian Flows, *ASME FED,* vol. 231/MD 66 (1995) 99-105.

[12] W. Duangthongsuk, S. Wongwises, Effect of thermophysical properties models on the predicting of the convective heat transfer coefficient for low concentration nanofluid, *International Communications in Heat and Mass Transfer* 35 (2008) 1320-1326.

[13] D.A. Nield, A.V. Kuznetsov, Thermal instability in a porous medium layer saturated by a nanofluid, *International Journal of Heat and Mass Transfer* 52 (2009) 5796-5801.

[14] E. Abu-Nada, H.F. Oztop, Effects of inclination angle on natural convection in enclosures filled with Cu-water nanofluid*, International Journal of Heat and Fluid Flow* 30 (2009) 669-678.

[15] D.A. Nield, A.V. Kuznetsov, The Cheng-Minkowycz problem for natural convective boundary-layer flow in a porous medium saturated by a nanofluid, *International Journal of Heat and Mass Transfer 52* (2009) 5792-5795.

[16] A.J. Chamkha, A.M. Aly, H. Al-Mudhaf, Laminar MHD mixed convection flow of a nanofluid along a stretching permeable surface in the presence of heat generation or absorption effects, *International Journal of Microscale and Nanoscale Thermal and Fluid Transport Phenomena*, 2010.

[17] A.J. Chamkha, R.S.R. Gorla, K. Ghodeswar, Non-similar solution for natural convective boundary layer flow over a sphere embedded in a porous medium saturated with a nanofluid, *Transport in Porous Media*, 86 (2011) 13-22.

[18] Rama Subba Reddy Gorla, S.M.M. EL-Kabeir, A.M. Rashad, Heat transfer in the boundary layer on a stretching circular cylinder in a nanofluid, *Journal Of Thermophysics And Heat Transfer*, 25 (2011) 183-186.

[19] R.H. Christopher and S. Middleman, Power-law flow through a packed tube, *I and EC Fundamentals* 4 (1965) 422-426.

[20] R.V. Dharmadhikari and D.D. Kale, Flow of non-Newtonian fluids through porous media, *Chemical Eng. Sci.* 40 (1985) 527-529.

[21] F. G. Blottner, Finite-difference methods of solution of the boundary-layer equations, *AIAA Journal* 8 (1970) 193-205.

Received 26 November 2010; received in *revised* form 11 September 2011; accepted 13 September 2011.